Image Color Mapping in Complex Log Space

Hiroaki Kotera; Kotera Imaging Laboratory, Chiba, Japan

Abstract

This paper proposes a cluster-to-cluster image color transform algorithm. Recently, Suntory Flowers announced the development of world's first blue rose "APPLAUSE". Since roses lack the blue pigment, it was long believed to be impossible. The key to success lies in the introduction of blue gene from pansy into rose. In the previous paper, PCA matching model was successfully applied to a seasonal color change in flowers, though it's not real but virtual. However, the tonal color transitions between the different color hues such as red rose and blue pansy were not so smooth but unnatural because of spatially independent color blending. In addition, the clear separation of blue or purple petal colors from greenish backgrounds is not always easy too. The paper improves the color transform algorithm in the two points, firstly, the clear color separation by introducing a "complex log" color space and secondly, the smoothed tonal color transition by introducing a "time-variant" matrix for PCA matching. The proposed algorithm is applied to ROI (Region Of Interest) image color transform, for example, a blue rose creation from red rose by continuous color stealing of pansy blue.

Introduction

Image segmentation plays an important role in many applications. Color clustering is a low-level task in the first stage of color image segmentation. The color of nature changes with passing time. Natural images are composed of clustered color objects with similarity to be shared each other. A concept of color transfer between two images was introduced by Kotera's PCA matching model [1] and advanced by Reinhard [2] as "scene color transfer" model. "Color stealing" by Barnsley [3] was a new concept of Fractal-based color sharing and used for synthesizing a new image by picking up a region color in one image and moving it into another image. Mochizuki [4] applied this idea to CG as "stealing autumn color". Our previous papers [5][6] extended the PCA matching model to a time-variant color transform and applied to imitate a seasonal color change in flowers. The model worked well for transferring a petal color in the source image into a different petal color in the target image, provided that the hue change between the source and target petal clusters is gentle.

Recently, Suntory Flowers succeeded in the development of world's first blue rose "APPLAUSE". Since roses lack the blue pigment, it was long believed to be impossible. The key to success lies in the introduction of blue gene from pansy into a source rose. Hearing this exciting news, we tested the PCA matching model to create a bluish rose from reddish roses by stealing a pansy blue. Of course, it's not a real but a virtual flower. Though, the color transitions in hue and tone were not so smooth but unnatural when the source and target images have a large difference in their color tones. This unnaturalness comes from the spatially-independent color blending between source and target clusters. In addition, it's not always easy to separate a dull-hued bluish or purple petal clearly distinguishing from the greenish background.

This paper improves the color stealing algorithm by introducing the new ideas of

a) Complex "*Log-Polar Transform* (*LPT*)" for clear segmentation of petal area by k-means clustering.
b) "*Time-variant PCA matching matrix*" for smoothed color transitions from source to target.

Fig.1 overviews the proposed color stealing model and its application to creating a unique bluish rose from red, pink, orange, or yellow roses.

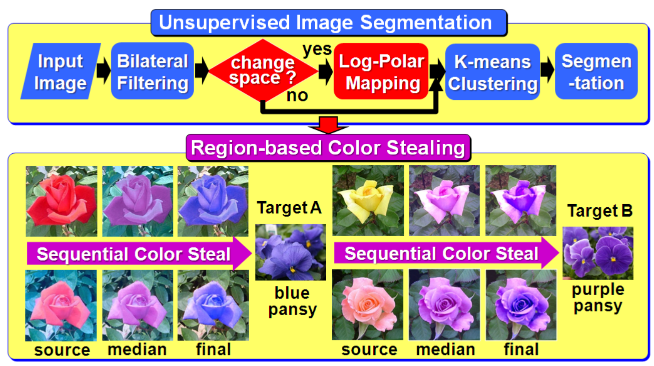

Figure 1 *Overview of segmentation-based color stealing model*

Spatial Pre-Filtering for K-means Clustering

In practice, *k-means* clustering has been conveniently used for unsupervised image segmentation. Since *k-means* has a drawback in nonuse of spatial information, *JSEG* [7] introduced an excellent post-processing of region growing and region merging to avoid over segmentations for the textural areas. Instead of post-processing, this paper introduces a joint spatial-range bilateral filter before *k-means* clustering to make smooth the textures.

Joint LAB-Range Bilateral Filter

Before segmentation, {L^*, a^*, b^*} images are pre- processed by a *bilateral filter* to make the *"texture"* area smooth without degrading the edge sharpness as shown in ***Fig.2***.
The filtered pixel value $I_F(\boldsymbol{q})$ at central position $\boldsymbol{q}$ is given as a weighted sum of its surround pixels at $\boldsymbol{p}$, where the spatial filter G_S works active or inactive if the range filter G_R has a high value for the low-gradient areas or a low value for the high-gradient edges.

$$I_F(\boldsymbol{q}) = \frac{1}{K(\boldsymbol{q})} \sum_{p \subset \Omega} G_S(\|\boldsymbol{p}-\boldsymbol{q}\|) G_R(|I(\boldsymbol{p}) - I(\boldsymbol{q})|) I(\boldsymbol{p})$$
$$\text{where, } K(\boldsymbol{q}) = \sum_{p \subset \Omega} G_S(\|\boldsymbol{p}-\boldsymbol{q}\|) G_R(|I(\boldsymbol{p}) - I(\boldsymbol{q})|) \tag{1}$$
$$\text{and } G_S(\boldsymbol{x}) = exp\left\{-\frac{(\boldsymbol{x})^2}{2\sigma_S^2}\right\},\ G_R(\boldsymbol{x}) = exp\left\{-\frac{(\boldsymbol{x})^2}{2\sigma_R^2}\right\}$$

Here, $I(\boldsymbol{p})=L^*(\boldsymbol{p})$, $a^*(\boldsymbol{p})$, $b^*(\boldsymbol{p})$ at pixel position $\boldsymbol{p}$ is assigned for each image plane of {L^*, a^*, b^*}.

In comparison with normal k-means, the pre-processing bilateral filter clearly improves the segmentation accuracy. The typical rose images with vivid colors are mostly well segmented by the proposed K-means in normal CIELAB space as shown in ***Fig.3***.

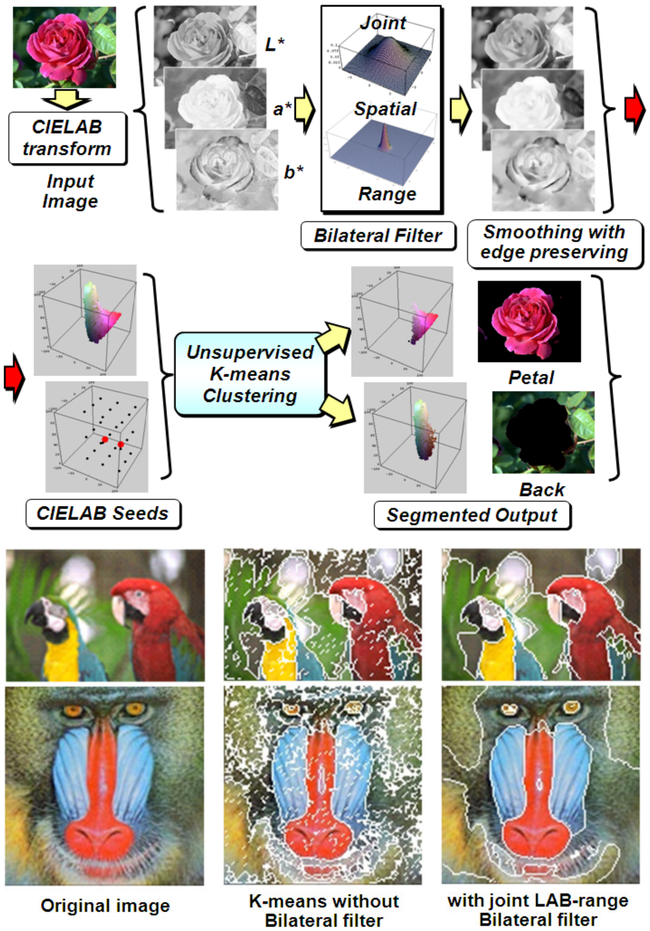

Figure 2 *K-means clustering with Bilateral filtering*

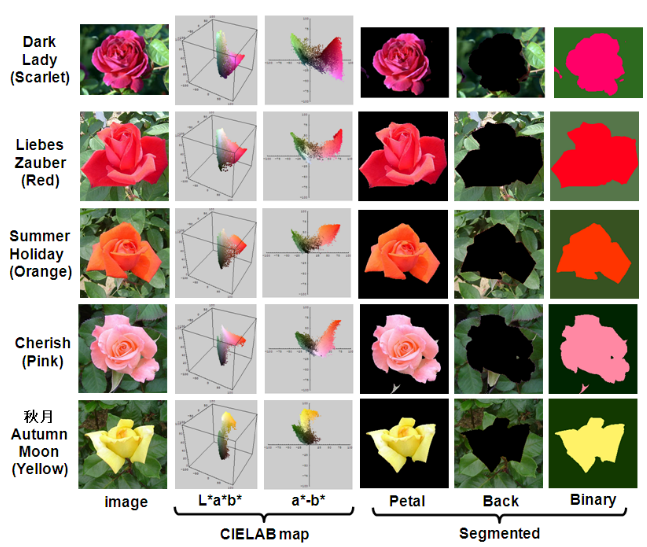

Figure 3 *Segmentation results in typical roses by proposed K-means*

Clustering in Complex Log-Polar Space

Motivation for Using Log-Polar Transform

Although the vivid colored roses are mostly well segmented to their petal and the background in normal CIELAB space, the LPT is selected for the dull-hued roses as the occasion demands.

Schwartz's complex Log-Polar Transform (LPT) [8] is known as a topographic mapping model of visual field onto the cortex. Though LPT is a space-variant image encoding scheme used in computer vision, here it's tested for the better separation of the clustered color objects from a point of mapping features of LPT.

Two-dimensional LPT function maps a complex number z to another complex number $log\,(z)$ as

$$z = x + jy = \rho e^{j\theta}\,;\ \rho = |z| = \sqrt{x^2 + y^2}\,,\ \theta = tan^{-1}(y/x) \quad (2)$$

$$log(z) = u + jv = log(\rho) + j\,\theta;\ j = \sqrt{-1} \quad (3)$$

It maps the Cartesian coordinates (x, y) to the log-polar space notated as (u, v).

Since the origin itself is a singularity, the CBS (Central Blind Spot) model is introduced not to have the negative radii by setting the blind spot size $\rho \geq \rho_0$ as

$$(u,\ v) \triangleq (log_a(\rho/\rho_0),\ \theta) \quad (4)$$

Considering the discrete *log-polar* space with R rings and S sectors for integer numbers of u=1, 2, …, R and v=1, 2, …, S, we get the following relations [9] as

$$a = exp[log(\rho_R/\rho_0)/R] \quad (5)$$

$$\Delta\rho = \rho_u - \rho_{u-1} = \rho_0 a^{u-1}(a-1) \quad (6)$$

$$\Delta\theta = \theta_v - \theta_{v-1} = 2\pi/S\,;\ \theta_v = v\Delta\theta \quad (7)$$

Since the source points (x, y) in a sector area $(\Delta\rho(u),\ \Delta\theta)$ are mapped to the new coordinates (u, v), points on the circles around the origin with equal radii are placed at the parallel vertical lines. While, points on the lines outward from the origin separated by equal angle are mapped onto the parallel horizontal lines.

Now assigning the (x, y) coordinates to the (a^*, b^*) values, the colors on the linear line with the same hue angle are mapped to the same horizontal line and shifted to the vertical directions for the different hue angles. As well, the colors on the circle with the same chroma (radius) are mapped to the same vertical line and shifted to the horizontal directions for the different radii.

Complex Log-Polar Transform in CIELAB Space

Applying the LPT to CIELAB color space, Eq. (4) is given by

$$z = a^* + jb^* = \rho e^{j\theta}\,;\ \rho = \sqrt{a^{*2} + b^{*2}}\,,\ \ \theta = tan^{-1}(b^*/a^*) \quad (8)$$

Where, angle θ denotes the color hue in uniform perceptual color space CIELAB.

L^* value is also converted to the same *logarithmic* scale with the offset bias μ as

$$w = log(L^* + \mu) \quad (9)$$

Now, $\{L^*,\ a^*,\ b^*\}$ colors are mapped to the new complex LPT space $\{w,\ u,\ v\}$.

About Log Scale and Hue Continuity in LPT

Two simple questions maybe arise for the use of LPT. One is why the Log scale in the radius ρ is useful. Both of Log-Polar and Linear-Polar transforms have been examined in the experiments. The other is a risk that any split in the single color cluster may happen across the hue angle θ=0 and θ=2π. To avoid the split, $\pi/2$ shift (rotation) of hue angle is selectively performed on the image for crossing the a^* axis (headed 4th to 1st quadrant).

Complex Log-Polar vs. Linear-Polar Transforms

Fig.4 **(*a*)** compares the color mapping results for Munsell color chips from normal CIELAB to complex Linear-Polar and Log-Polar spaces. It's shown that the color chips with similar hues tend to be mapped onto the horizontal lines separated vertically depending on their hue angles and the chips with similar chromas onto the vertical lines separated horizontally depending on their chroma values. ***Fig.4*** **(*b*)** is a result for dull-hued images.

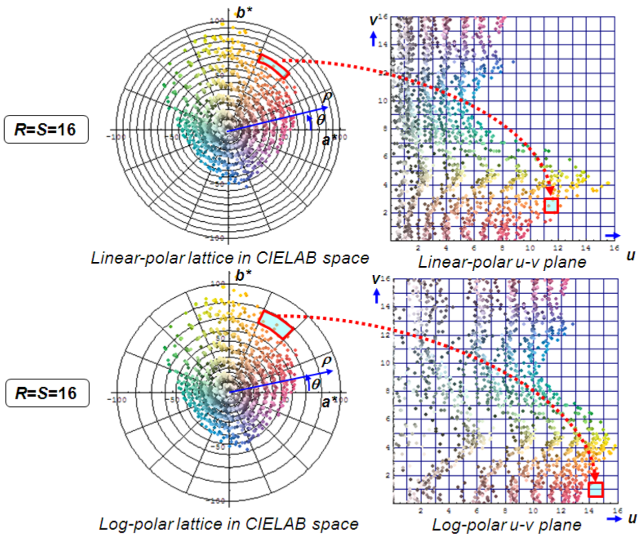

(a) *Color mapping for Munsell chips* (*1600 colors*)

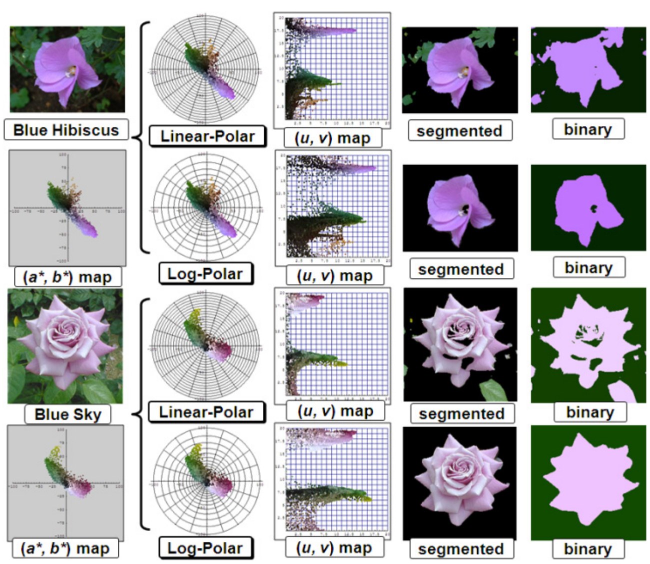

(b) *Mapping and segmentation results for dull-hued rose mages*(***R=S=20***)

Figure 4 *Comparison of mapping in Linear-polar vs. Log-polar spaces*

When the image colors are remapped onto complex LPT, their clusters are occasionally relocated to the easier segmentation. ***Fig.4*** **(*b*)** shows the segmentation results for dull-hued bluish petals in comparison with normal CIELAB vs. Linear-Polar and Log-Polar spaces. In these samples, the petals are better segmented in the complex Log-Polar than complex Linear-Polar space in case of smaller numbers of rings and sectors, for example, R=S=20 or less. As the number of R and S increase, the lattice in (ρ, θ) coordinates is divided finer and the Linear-Polar resulted in much the same performance as the Log-Polar for R=S=100. Since CIELAB itself is a well-designed uniform color space with cube-root nonlinearity, it may be questionable to apply the logarithmic transform moreover. Of course, the complex Log-Polar transform is not always superior to normal CIELAB but dependent on the image. We need any criterion to judge which space has the better separability for the given color clusters.

Cluster Separability

As a measure of goodness in clustering, the invariant criterion function is estimated based on the scatter matrices [10] as follows. The scatter matrix for the *k-th* cluster in subset $\boldsymbol{D}_k$ is described as

$$\boldsymbol{S}_k = \sum_{\boldsymbol{x}\in \boldsymbol{D}_k} (\boldsymbol{x}-\boldsymbol{m}_k)(\boldsymbol{x}-\boldsymbol{m}_k)^t \ ; \ \boldsymbol{m}_k = \frac{1}{N_k} \sum_{\boldsymbol{x}\in \boldsymbol{D}_k} \boldsymbol{x} \tag{10}$$

Where, N_k denotes the number of pixels in class k.
The within-cluster scatter matrix $\boldsymbol{S}_W$ is given by the sum of $\boldsymbol{S}_k$ as

$$\boldsymbol{S}_W = \sum_{k=1}^{K} \boldsymbol{S}_k \tag{11}$$

While, the between–cluster scatter matrix $\boldsymbol{S}_B$ is defined by

$$\boldsymbol{S}_B = \sum_{k=1}^{K} N_k (\boldsymbol{m}_k - \boldsymbol{m})(\boldsymbol{m}_k - \boldsymbol{m})^t \ ; \ \boldsymbol{m} = \frac{1}{N}\sum_{\boldsymbol{x}\in \boldsymbol{D}} \boldsymbol{x} = \frac{1}{N}\sum_{k=1}^{K} N_k \boldsymbol{m}_k \tag{12}$$

The total scatter matrix $\boldsymbol{S}_T$ is the sum of $\boldsymbol{S}_W$ and $\boldsymbol{S}_B$ as given by

$$\boldsymbol{S}_T = \sum_{\boldsymbol{x}\in \boldsymbol{D}} (\boldsymbol{x}-\boldsymbol{m})(\boldsymbol{x}-\boldsymbol{m})^t = \boldsymbol{S}_W + \boldsymbol{S}_B \tag{13}$$

Note that $\boldsymbol{S}_T$ doesn't depend on how the set of samples is partitioned into clusters. The between-cluster scatter $\boldsymbol{S}_B$ goes up as the within-cluster $\boldsymbol{S}_W$ goes down. Now, we can define an optimum partition as the criterion that minimizes $\boldsymbol{S}_W$ or maximizes $\boldsymbol{S}_B$.

The criterion function for the cluster separability is defined by

$$J_{B/W} = T_{race}\left[\boldsymbol{S}_W^{-1} \boldsymbol{S}_B\right] = \sum_{i=1}^{3} \lambda_i \ ; \ \lambda_i \ \textit{is the } i-th\textit{. eigenvalue} \tag{14}$$

Improved Clustering Results in Complex LPT

The *complex* LPT may be selected for the dull-hued roses as the occasion demands. ***Fig.5*** shows a comparative sample for the segmentation in normal CIELAB space vs. complex Linear-Polar and Log-Polar transforms with the cluster separability of $\boldsymbol{J}_{B/W}$.

The petal areas are clearly segmented by applying complex Linear-Polar and Log-Polar transforms better than normal CIELAB space with the higher $\boldsymbol{J}_{B/W}$ values. The performances by complex Linear-Polar and Log-Polar transforms are much the same for "*Blue rose AppLause*" and *"Hybrid Tea Rose"*, while Log-Polar is little bit superior to Linear-Polar for "*Blue moon*".

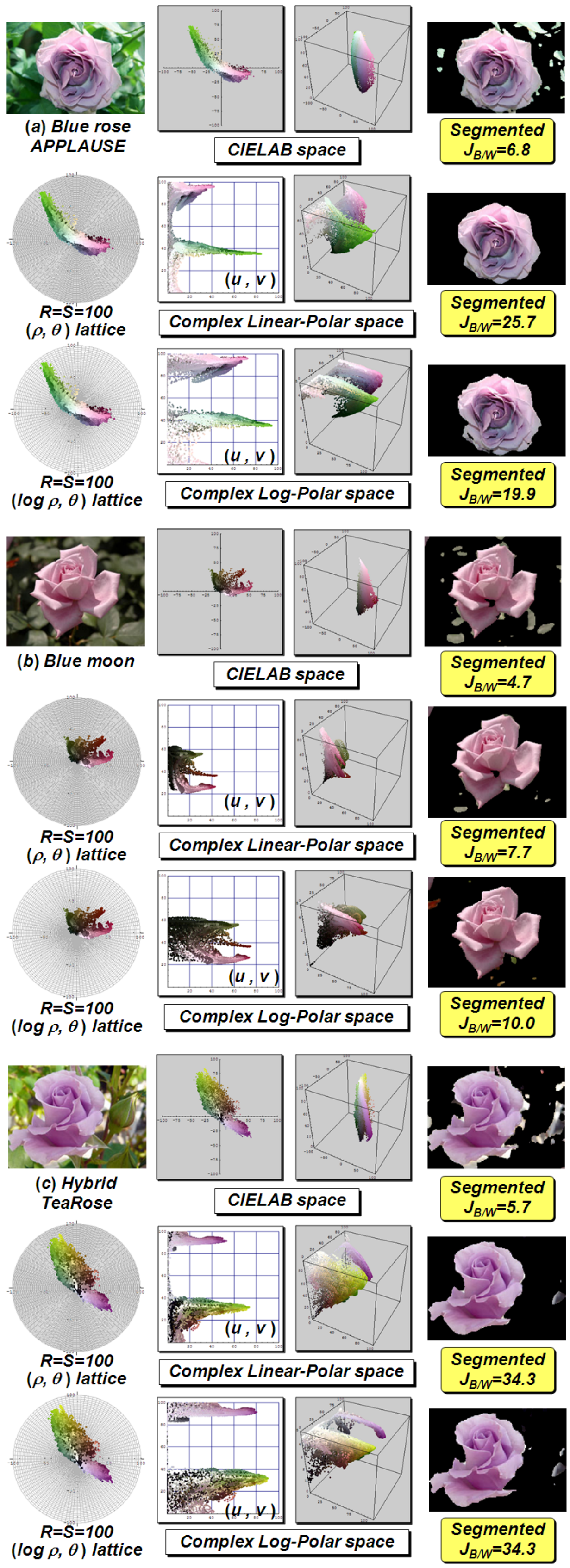

Figure 5 *Comparison in CIELAB vs. complex Linear- and Log-Polar spaces*

Region-based Color Stealing

The proposed color clustering method is applied to a Segmentation-based cluster-to-cluster color transfer between two different images. The paper introduces a color stealing application for rose flowers.

Cluster-to-Cluster Principal Component Matching

The key to color transfer between two different segmented objects in source and target images is based on "cluster-to-cluster" PCA color matching algorithm [11] as follows.

First, the source color vector ${}_S\boldsymbol{X}$ in image $\boldsymbol{S}$ and the target color vector ${}_D\boldsymbol{X}$ in image $\boldsymbol{T}$ are projected onto the vectors ${}_S\boldsymbol{Y}$ and ${}_T\boldsymbol{Y}$ in the common PC space by Hotelling Transform as

$$\begin{aligned} &{}_S\boldsymbol{Y}={}_S\boldsymbol{A}({}_S\boldsymbol{X}-{}_S\boldsymbol{\mu}),\ \ {}_T\boldsymbol{Y}={}_T\boldsymbol{A}({}_T\boldsymbol{X}-{}_T\boldsymbol{\mu}) \\ &{}_S\boldsymbol{\mu} = E\{{}_S\boldsymbol{X}\},\ \ {}_T\boldsymbol{\mu} = E\{{}_T\boldsymbol{X}\}\ :\text{mean vectors} \end{aligned} \tag{15}$$

${}_S\boldsymbol{A}$ and ${}_T\boldsymbol{A}$ are the eigen vectors of covariance matrices ${}_S\boldsymbol{C}_X$ and ${}_T\boldsymbol{C}_X$ for ${}_S\boldsymbol{X}$ and ${}_T\boldsymbol{X}$.
Thus the covariance matrices ${}_S\boldsymbol{C}_Y$ and ${}_T\boldsymbol{C}_Y$ for ${}_S\boldsymbol{Y}$ and ${}_T\boldsymbol{Y}$ are diagonalized in PC space as given by

$$\begin{aligned} &{}_S\boldsymbol{C}_Y={}_S\boldsymbol{A}({}_S\boldsymbol{C}_X){}_S\boldsymbol{A}^t = diag\{{}_S\lambda_1,\ {}_S\lambda_2,\ {}_S\lambda_3\} \\ &{}_T\boldsymbol{C}_Y={}_T\boldsymbol{A}({}_T\boldsymbol{C}_X){}_T\boldsymbol{A}^t = diag\{{}_T\lambda_1,\ {}_T\lambda_2,\ {}_T\lambda_3\} \end{aligned} \tag{16}$$

Where, $\{{}_S\lambda_i\}$ and $\{{}_T\lambda_i\}$ are the eigen values of ${}_S\boldsymbol{Y}$ and ${}_T\boldsymbol{Y}$.

Second, the source color vector ${}_S\boldsymbol{Y}$ and the target color vector ${}_T\boldsymbol{Y}$ are mapped onto the same PC axes and ${}_S\boldsymbol{Y}$ is transformed to match ${}_T\boldsymbol{Y}$ by the scaling matrix ${}_S\boldsymbol{S}_T$ as follows.

$$\begin{aligned} &{}_T\boldsymbol{Y} = ({}_S\boldsymbol{S}_T)\cdot({}_S\boldsymbol{Y}), \\ &{}_S\boldsymbol{S}_T = diag\left\{\sqrt{{}_T\lambda_1/{}_S\lambda_1},\sqrt{{}_T\lambda_2/{}_S\lambda_2},\sqrt{{}_T\lambda_3/{}_S\lambda_3}\right\} \end{aligned} \tag{17}$$

Connecting Eq. (15) to Eq. (17), the colors $\{{}_S\boldsymbol{X}\}$ in the source cluster $\boldsymbol{S}$ is transformed to the set of destination colors $\{{}_D\boldsymbol{X}\}$ that is approximately matched to the colors $\{{}_T\boldsymbol{X}\}$ in the target cluster $\boldsymbol{T}$ by the matrix $\boldsymbol{M}_C{}^7$. $\boldsymbol{M}_C$ matches the color hue by cluster rotation and the variance by scaling as

$$\begin{aligned} &{}_D\boldsymbol{X} = \boldsymbol{M}_C({}_S\boldsymbol{X}-{}_S\boldsymbol{\mu})+{}_T\boldsymbol{\mu}\cong{}_T\boldsymbol{X} \\ &where,\ \ \boldsymbol{M}_C = ({}_T\boldsymbol{A}^{-1})({}_S\boldsymbol{S}_T)({}_S\boldsymbol{A}) \end{aligned} \tag{18}$$

Time-variant PCA Matching to Blended Clusters

In the previous paper [5][6], the PCA matching model is applied to a time-variant sequential color transfer to imitate a seasonal color change in flowers. A most simple way for time-variant color transfer is to use cross dissolving [10] which creates a time-varying median image $\boldsymbol{R}$ by stealing the pixels from target $\boldsymbol{T}$ by the ratio of α_n and blending them with the source $\mathbf{S}$ by the ratio of $(1\text{-}\alpha_n)$ as follows.

$$\boldsymbol{R}(n) = (1-\alpha_n)\boldsymbol{S} + \alpha_n\boldsymbol{T}\ \ for\ \ \alpha_n = n/N\ ;\ n = 0,1,\cdots,N \tag{19}$$

But, the cross dissolving causes a double exposure artifacts due to the mixture of independent pixels in $\boldsymbol{S}$ and $\boldsymbol{T}$. While, the PCA matching algorithm is applied to time-variant color change from $\boldsymbol{S}$ to $\boldsymbol{T}$ by just substituting the blended cluster $\boldsymbol{R}$ for the target $\boldsymbol{T}$. The petal color in source $\boldsymbol{S}$ is changed gradually approaching to that in the blended cluster $\boldsymbol{R}$ without double exposure artifacts, because the color transfer is limited to the segmented areas in ***S*** and ***T***.

Though this model works well for the images with the similar color hues, unfortunately, the tonal color transfer is not always smooth between the big hue difference such as red to/from blue.

Time-variant PCA Matching Matrix

An improved algorithm is proposed to make the color transitions more smoothly between the clusters with big hue differences. Instead of time-variant color blending function by Eq. (19), a time-variant color matching matrix is introduced.

Here, the *matrix* $\boldsymbol{M_C}$ is modified to be variable according to the time-variant ratio of α_n as

$$\boldsymbol{M}_C(n) = (1-\alpha_n)\boldsymbol{I} + \alpha_n \boldsymbol{M}_C \quad for\ \alpha_n = n/N;\ n = 0,1,\cdots,N \tag{20}$$

$\boldsymbol{M_C}(n)$ changes from $\boldsymbol{I}$ to $\boldsymbol{M_C}$ according to the time sequence n=0 ~ 1, where $\boldsymbol{I}$ denotes 3 x 3 identity matrix.

Substituting $\boldsymbol{M_C}(n)$ for $\boldsymbol{M_C}$ in Eq. (18), the colors $\{{}_S\boldsymbol{X}\}$ in the source cluster $\boldsymbol{S}$ is transformed to the destination colors $\{{}_D\boldsymbol{X}\}$ with time sequence n, finally matching to the colors $\{{}_T\boldsymbol{X}\}$ in the target cluster $\boldsymbol{T}$ like as

$${}_D\boldsymbol{X} = \{(1-\alpha_n)\boldsymbol{I} + \alpha_n \boldsymbol{M}_C\}({}_S\boldsymbol{X} - {}_S\boldsymbol{\mu}) + {}_T\boldsymbol{\mu} \quad where,\ \boldsymbol{M}_C = ({}_T\boldsymbol{A}^{-1})({}_S\boldsymbol{S}_T)({}_S\boldsymbol{A}) \tag{21}$$

Fig.6 illustrates the basic concept of time-variant PC matching matrix model for cluster-to-cluster color stealing application.

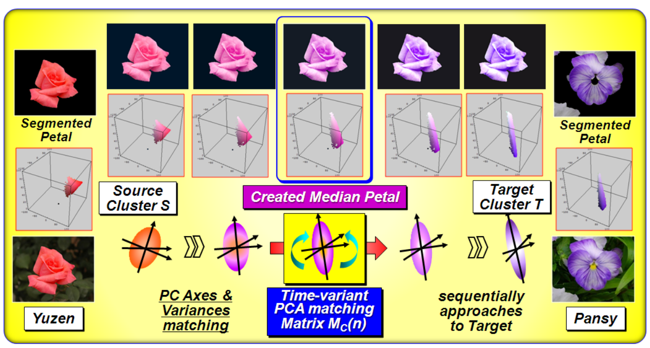

Figure 6 *Time-variant PCA color matching matrix model*

Blue Rose Creation by Stealing Pansy Blue

In 2004, Suntory Flowers Limited announced the successful development of the world's first blue rose "APPLAUSE", with nearly 100% blue pigment in the petals. Because roses lack blue pigment, their biotechnology research since 1990, introduced a blue gene from pansies into roses.

Now the proposed time-variant PC matching matrix model is applied to create a blue rose from a red rose by stealing the bluish colors from pansy as same as Suntory, though this is, of course, not a real but virtual simulation.

The results are compared with the popular conventional cross resolving method and our previous time-variant blending model The proposed time-variant PC matching matrix model clearly resulted in the smoother color transitions in the hue and gradation of intermediate (median) image sequences (see ***Fig.7***).

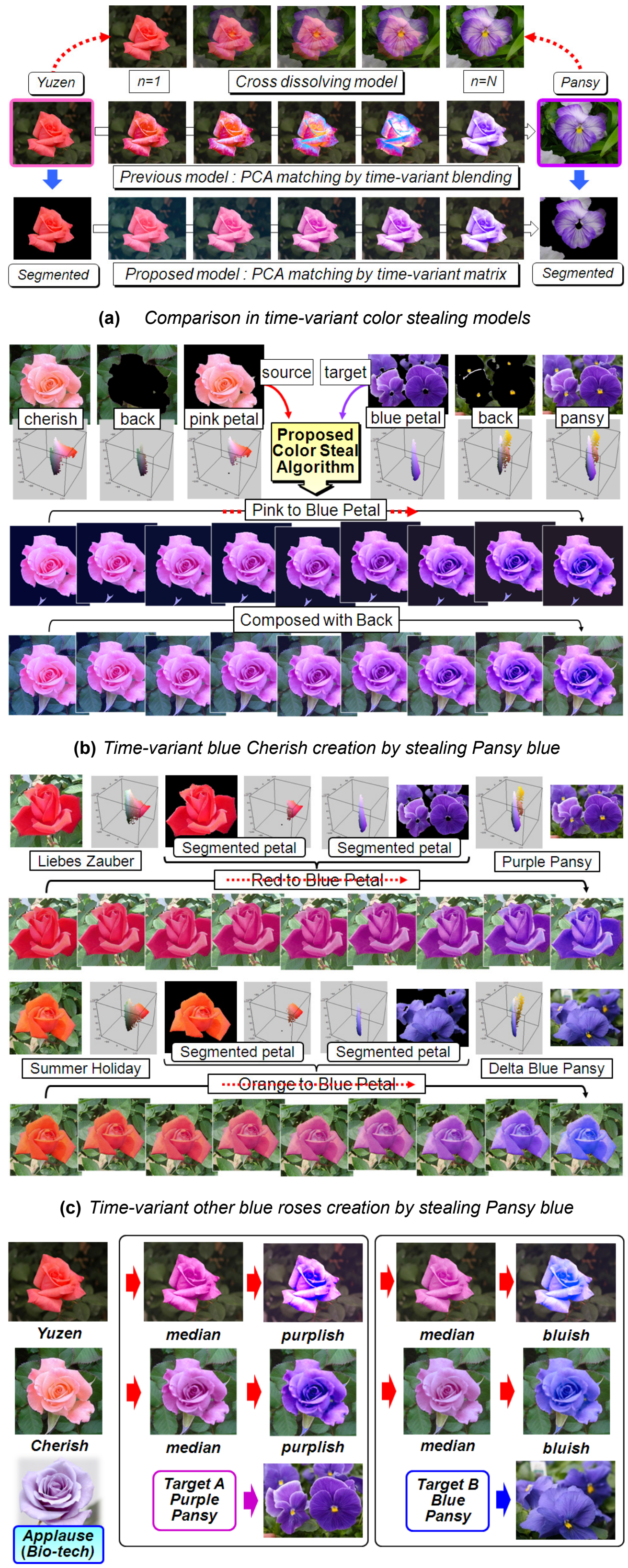

(d) *Created different blue roses by stealing two types of pansy blues*

Figure 7 *Creation of blue roses by stealing Pansy blues*

Conclusions

The paper proposed a novel approach to a segmentation-based ROI image color transformations. Image segmentation is the basis for Computer Vision, but there is no royal road to the unsupervised clustering method for unknown color objects. K-means clustering is a most popular algorithm for separating the color object with unique surface-color-hue without any learning samples.

Firstly, the pre-processing by joint LAB-range bilateral filtering proved to be very effective for separating the petal area from the complex background.

Secondly, paying our attention to the hue-oriented image color distributions, the color separability in clusters is newly discussed from a point of Schwartz's complex LPT mapping. Since the pixel colors on the same linear hue lines with different hue angles are mapped onto the same horizontal lines but separated vertically, such color clusters are remapped to be more separable. Although the LPT is a well-known space-variant image encoding scheme useful for computer vision sytem but hasn't any meaningful relation to the geometrical design in color space, it resulted in the distinct cluster separability for the segmentation of dull-hued cold color roses better than the normal CIELAB space. The invariant criterion on the cluster separability is estimated by using the scatter matrices and the complex Log-polar outperforms Linear-polar in case of small number of rings, R in the ρ direction.

However, the k-means clustering in LPT space is not always superior to normal CIELAB but is image-dependent. In order to switch on/off the LPT according to the image color distribution, a simple and quick pre-estimation tool for the cluster separability is desirable to be developed and is left behind as a future work.

Lastly, the segmentation-based cluster-to-cluster PCA color matching algorithm has advanced by introducing a time-variant matching matrix, coupled with complex LPT mapping scheme. The proposed color stealing model is successfully applied to a time-variant virtual blue rose creation from usual reddish or warm color roses, resulting in the smoothed color transitions.

References

[1] H. Kotera et al, Object-oriented Color Matching by Image Clustering, Proc. CIC6, 154-158, 1998

[2] E. Reinhard et al, Color transfer between images, Proc.IEEE Comp. Graph. Appl., 34-40, Sep/Oct., 2001

[3] M. Barnsley, Super Fractals, Cambridge Press, 2006

[4] S. Mochizuki et al, Stealing Autumn Color, SIGGRAPH, 2005

[5] H. Kotera, Sequential Color Stealing of SOUVENIR D'ANNE FRANK, Proc. AIC2009, 2009

[6] Hiroaki Kotera, Morphological Color Change in Morning Glory, Proc. CIC17, 79-84, 2009

[7] Y. Deng and B. S. Manjunath, IEEE Trans. Patt. Anal. Machine Intell., 23, 9, 800-810, 2001

[8] E. L. Schwartz, Spatial Mapping in the Primate Sensory Projection: Analytic Structure and Relevance to Perception, Biological Cybernetics, 25, 181-194, 1977

[9] J. V. Traver and F. Pla, Designing the lattice for log-polar images, Proc. 11th DGCI, 164-173,2003

[10] R. O. Duda, P. E. Hart, and D. G. Stork, Pattern Classification, John-Wiley & Sons, Inc., NY, 2001

[11] H. Kotera and T. Horiuchi, Automatic Interchange in Scene Colors by Image Segmentation, Proc. CIC12, 93-99, 2004

[12] M. Grundland et al, Cross Dissolve without Cross Fade, Eurographics'06, 25, 3, 2006

Author Biography

Hiroaki Kotera *joined Panasonic Co., in 1963. He received Doctorate from Univ. of Tokyo. After worked in image processing at Matsushita Res. Inst. Tokyo during 1973-1996, he was a professor at Dept. Information and Image Sciences, Chiba University until his retirement in 2006. He received 1993 journal award from IS&T, 1995 Johann Gutenberg prize from SID, 2005 Chester Sall award from IEEE, 2006 journal award from ISJ and 2008 journal award from SPSTJ. He is a Fellow of IS&T.*